

A Single-phase Harmonics Extraction Algorithm Based on the Principle of Trigonometric Orthogonal Functions

Hao Yi[†], Fang Zhuo^{*}, Feng Wang^{*}, Yu Li^{**}, and Zhenxiong Wang^{*}

^{†,*}State Key Laboratory of Electrical Insulation and Power Equipment, Xi'an Jiaotong University, Xi'an, China

^{**}Xi'an Spread Power Electric co., ltd., Xi'an, China

Abstract

For a single-phase active power filter (APF), designing a more efficient algorithm to guarantee accurate and fast harmonics extraction with a lower computing cost is still a meaningful topic. The common idea still employs a IRPT-based Park transform, which was originally designed for 3-phase applications. Therefore, an additional virtual signal generation (VSG) link is necessary when it is used in the single-phase condition. This method, with virtual signal generation and transform, is obviously not the most efficient one. Regarding this problem, this paper proposes a novel harmonics extraction algorithm to further improve efficiency. The new algorithm is based on the principle of trigonometric orthogonal functions (TOF), and its mathematical principle and physical meaning are introduced in detail. Its implementation and superiority in terms of computation efficiency are analyzed by comparing it with conventional methods. Finally, its effectiveness is well validated through detailed simulations and laboratory experiments.

Key words: Harmonics extraction, Single-phase active power filter, Trigonometric orthogonal functions

I. INTRODUCTION

One of the major changes in modern electrical systems is the fast-growing number of power electronics devices, whether in power generation side, transmitting side or end-user side. These nonlinear devices promote the level of power utilization. However, they also introduce serious power quality problems. One of these problems is harmonic current pollution. It distorts current waveforms and causes non-negligible power losses and even bus voltage pollution under some conditions, which greatly threatens the efficiency and performance of the whole system.

The shunt active power filter (APF) [1]-[3] is considered to be the most effective tool in dealing with harmonic current. In the latest studies [4], [5], its function is also introduced to distributed generators for multifunctional integration. It

cancel unwanted harmonics in load current by generating a corresponding opposite-phase harmonic current, leaving only the fundamental component in the source side.

The single-phase APF has attracted a lot of attention recently because of its great flexibility. Its general configuration can be illustrated as Fig. 1, whose control diagram includes the key parts of harmonics extraction, dc-voltage regulation, current tracking control and PWM generation. In this paper, emphasis is put on how to precisely and efficiently realize harmonics extraction.

Harmonics extraction is the basis of the APF and is also an old topic. An analogue method with a band-pass or low-pass circuit used to be an effective choice [6], [7], but it has been replaced by digital methods nowadays due to its limited precision.

For digital alternatives, the discrete Fourier transform (DFT) and its improved form, the fast Fourier transform (FFT)[8]-[11], provide accurate methods to realize selective harmonics extraction. However, their drawbacks of spectral leakage and slow response speed are non-negligible.

Some other intelligent harmonics extraction algorithms, such as fuzzy control [12], adaptive [13], [14], neural

Manuscript received Apr. 11, 2016; accepted Sep. 7, 2016

Recommended for publication by Associate Editor Jae-Do Park.

[†]Corresponding Author: yi_hao@xjtu.edu.cn

Tel: +86-02981330705, Xi'an Jiaotong University

^{*}State Key Laboratory of Electrical Insulation and Power Equipment, Xi'an Jiaotong University, China

^{**}Xi'an Spread Power Electric co., ltd, China

network [15]-[18] and phase-lock-loop (PLL) [19]-[21] based algorithms, also provide nice performances. However, their complexity is still a barrier for practical applications.

The Instantaneous Reactive Power Theory (IRPT) proposed by H. Akagi [22] is a widely-accepted option, which is normally for three-phase applications. It presents a clear physical meaning and accurate harmonic extraction results, and many other developed forms have been inspired by it [23]-[26]. However, cost computation is inevitable during Park transforms from the stationary frame to the synchronous rotation frame (SRF), especially when multiple harmonics are concerned. This drawback becomes more obvious in single-phase applications, because additional Virtual Signal Generation (VSG) link, realized by a Three-phase Signals Generation (TSG) or an Orthogonal Signal Generation (OSG) [27]-[30], is necessary to emulate a 3-phase condition to proceed the Park transforms. Obviously, this is not an efficient way for the single-phase applications. Extra resources need to be considered when designing digital signal processors to fulfill these additional computations.

Whether or not it is possible to further improve the efficiency of harmonics extraction algorithms for single-phase APF, it is still a meaningful research topic. This paper just focuses on this topic and a novel algorithm, based on Trigonometric Orthogonal Functions (TOF), is proposed. In addition to its accuracy, this novel method does not need any VSG link and is simpler to be realized than Park transforms, which makes it easier and more suitable for single-phase applications.

The principle of the proposed TOF-based algorithm is introduced from both the aspects of mathematics (in section II) and physical meaning (in section III). In addition, comparisons with conventional IRPT-based methods are given in section IV. Simulation and experimental results in section V validate the effectiveness of proposed algorithm. Finally, some conclusions are presented in section VI.

II. MATHEMATICAL PRINCIPLE

In mathematics, two different functions, whose inner product is zero, are called orthogonal. According to this concept, two trigonometric functions are orthogonal when the integral of their dot product becomes zero at $[-\pi, \pi]$. For instance, $\sin(\omega t)$ and $\cos(\omega t)$ are orthogonal functions, since:

$$\int_{-\pi}^{\pi} \sin(\omega t) \cdot \cos(\omega t) d(\omega t) = \frac{1}{2} \int_{-\pi}^{\pi} \sin(2\omega t) d(\omega t) = 0 \quad (1)$$

Similarly, $\sin(n\omega t + \varphi_n)$ and $\sin(k\omega t)$, as well as $\sin(n\omega t + \varphi_n)$ and $\cos(k\omega t)$, can also form orthogonal function pairs, respectively, as long as n and k are both integers and $n \neq k$. This paper just utilizes this principle, so-called TOF, to simplify the harmonics extraction algorithm for single-phase applications.

To further explain the utilization of TOF-based algorithm

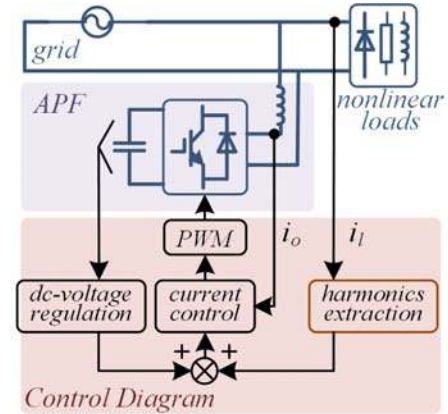


Fig. 1. General configuration of single-phase APF.

in harmonic extraction, a periodic distorted current $i(t)$ is expressed as (2), which is the sum of a set of sines according to the Fourier Series. For generality, the k^{th} order harmonic is assumed as the target to be extracted and is separately expressed in (2). It is:

$$i(t) = \left(\sum_{n=1}^N I_n \sin(n\omega t + \varphi_n) \right) + I_k \sin(k\omega t + \varphi_k) \quad (n \neq k) \quad (2)$$

where ω indicates the fundamental frequency in this paper; integer N is the highest order of the harmonic in $i(t)$; the subscripts n and k represent harmonics orders, but $n \neq k$; I_n and I_k mean the amplitudes of the n^{th} order and k^{th} order harmonics, respectively; and φ_n and φ_k imply the initial phase angles for the corresponding harmonics.

To extract the k^{th} order harmonic, $i(t)$ in (2) is multiplied by $\sin(k\omega t)$ as:

$$\begin{aligned} i(t) \cdot \sin(k\omega t) = & \\ & - \left(\sum_{n=1}^N \frac{I_n}{2} \left\{ \cos[(n+k)\omega t + \varphi_n] - \cos[(n-k)\omega t + \varphi_n] \right\} \right) \\ & - \frac{I_k}{2} \left[\cos(2k\omega t + \varphi_k) - \cos\varphi_k \right] \end{aligned} \quad (3)$$

Then calculate the mean value of doubled (3) at $[-\pi, \pi]$, i.e.

$$\begin{aligned} \frac{1}{2\pi} \int_{-\pi}^{\pi} i(t) \cdot \sin(k\omega t) d(\omega t) = & \\ \sum_{n=1}^N \frac{-I_n}{4\pi} \left\{ \underbrace{\int_{-\pi}^{\pi} \cos[(n+k)\omega t + \varphi_n] d(\omega t)}_0 - \underbrace{\int_{-\pi}^{\pi} \cos[(n-k)\omega t + \varphi_n] d(\omega t)}_0 \right\} & \\ - \frac{I_k}{4\pi} \underbrace{\int_{-\pi}^{\pi} \cos(2k\omega t + \varphi_k) d(\omega t)}_0 + \frac{I_k}{4\pi} \int_{-\pi}^{\pi} \cos\varphi_k d(\omega t) & \end{aligned} \quad (4)$$

Since n and k are both integers and $n \neq k$, it is always true that $n+k \geq 1$ and $|n-k| \geq 1$. Under this condition, the first three terms in (4) are all equal to zero, according to the principle of TOF. Therefore, expression (5) can be obtained by doubled (4), which is a time-invariant constant for given values of I_k and φ_k .

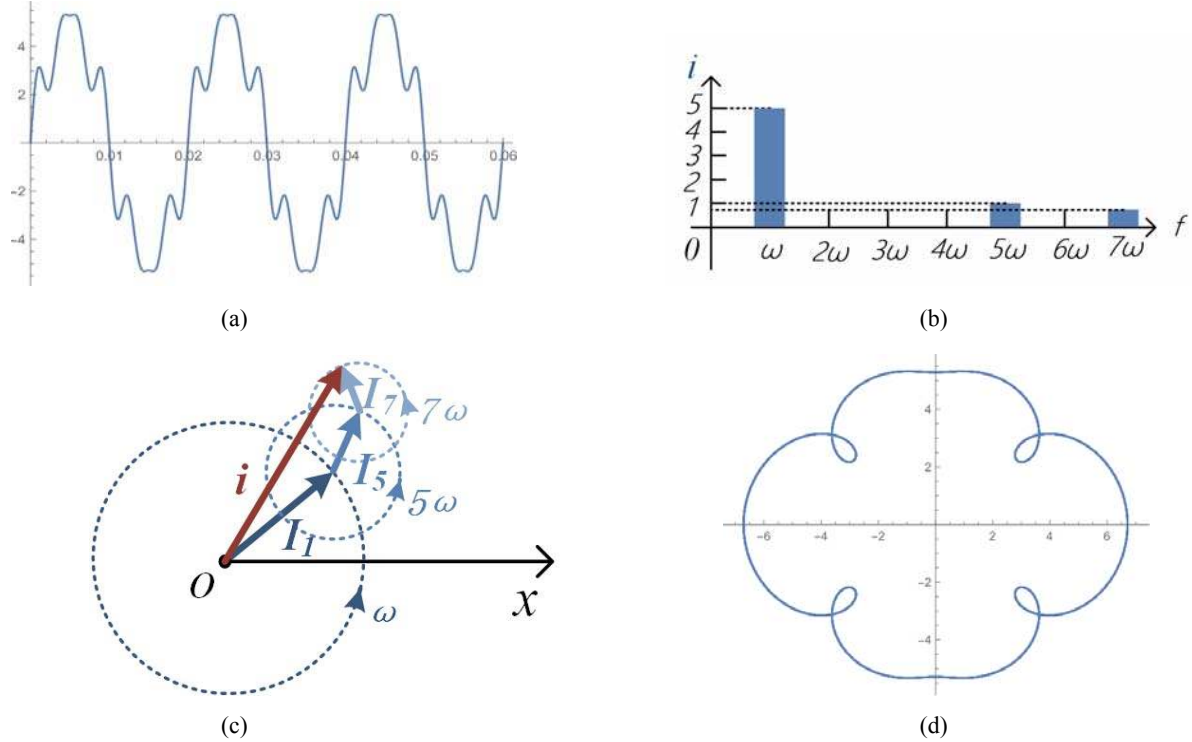


Fig. 2. Physical meaning illustrations of single-phase distorted current. (a) Waveform. (b) Harmonic spectrum. (c) Vectors construction in the polar coordinate. (d) Moving trajectory in the polar coordinate.

$$\frac{1}{\pi} \int_{-\pi}^{\pi} i(t) \cdot \sin(k\omega t) d(\omega t) = I_k \cos \varphi_k \quad (5)$$

Similarly, by multiplying $\cos(k\omega t)$ by $i(t)$ in (2) and then calculating its mean value at $[-\pi, \pi]$, expression (6) can be obtained, which is also a time-invariant constant for given values of I_k and φ_k .

$$\frac{1}{\pi} \int_{-\pi}^{\pi} i(t) \cdot \cos(k\omega t) d(\omega t) = I_k \sin \varphi_k \quad (6)$$

Afterwards, the k^{th} order harmonic can be restored by summing up the multiplication of (5) with $\sin(k\omega t)$ and the multiplication of (6) with $\cos(k\omega t)$, which is:

$$\begin{aligned} i_k(t) &= I_k \cos \varphi_k \cdot \sin(k\omega t) + I_k \sin \varphi_k \cdot \cos(k\omega t) \\ &= I_k \sin(k\omega t + \varphi_k) \end{aligned} \quad (7)$$

Compared with (2), the result in (7) is just the target of k^{th} order harmonic, which validates the mathematical process above. And this mathematical process is named the TOF-based algorithm in this paper. In summary, the whole process from (3) to (7) can be expressed as:

$$\begin{aligned} I_k \sin(k\omega t + \varphi_k) &= \sin(k\omega t) \cdot \frac{1}{\pi} \int_{-\pi}^{\pi} i(t) \cdot \sin(k\omega t) d(\omega t) \\ &+ \cos(k\omega t) \cdot \frac{1}{\pi} \int_{-\pi}^{\pi} i(t) \cdot \cos(k\omega t) d(\omega t) \end{aligned} \quad (8)$$

It is worth noting that the result in (8) does not change if $\sin(k\omega t)$ and $\cos(k\omega t)$ are replaced by $\sin(k\omega t + \varphi_x)$ and $\cos(k\omega t + \varphi_x)$, respectively, as long as the same φ_x is ensured. This means that the harmonic frequency, instead of the exact

actual phase information, is sufficient to extract the concerned harmonic with the TOF-based method, which further decreases the demands of the PLL link.

III. PHYSICAL MEANING

Unlike the three-phase signals that rotate in the $\alpha\beta$ frame, the single-phase distorted current, with the Fourier Series form in (2), can be directly illustrated in the polar coordinate, with its moving trajectory rotating as Fig. 2. The current vector is formed by head-to-tail-connected harmonic vectors, and each harmonic vector represents one harmonic component, which is rotating around its starting point, at the radius of the harmonic magnitude and at the speed of the harmonic angular frequency.

Taking a distorted current containing the 1st, 5th and 7th order components as an example, as depicted in Fig. 2(a) and (b), vectors i_1 , i_5 and i_7 represent the corresponding harmonics with the subscript indicating the order.

As shown in the Fig. 2(c), by setting the starting point of the vector i_1 as the origin point of the polar coordinate, its rotating trail is a circle with the radius I_1 and the rotating speed ω . Vector i_5 starts from the end point of i_1 , leaving a rotating circle at the radius I_5 and the speed 5ω from perspective of its own starting point. And similar situation takes place on the vector i_7 .

The entire distorted current, represented by the vector i , can be obtained through a sum of the vectors i_1 , i_5 and i_7 ,

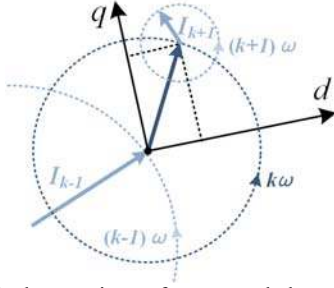


Fig. 3. Physical meaning of proposed harmonic extraction method.

leaving the trajectory as Fig. 2(d).

Please keep in mind that the aforementioned illustration is directly proceeded in the polar coordinate system, which is different from the $\alpha\beta$ frame for 3-phase signals. Therefore, it is more suitable for describing a single-phase signal. On this basis, a VSG link is not needed, and the TOF-based method, instead of Park transforms, can be employed to establish the rotating frame.

Based on the description above, the physical meaning of the TOF-based method can be introduced through Fig. 3, where the k^{th} order harmonic is assumed as the target for generality. According to section II, this method includes the three steps below:

A. Step 1, Establishing the Rotating Frame

This is realized by multiplying $\sin(k\omega t)$ and $\cos(k\omega t)$ with $i(t)$. As shown in Fig. 3, the established coordinate, named the dq frame, rotates counterclockwise at a speed of $k\omega$. From the view point of the dq frame, each order component in $i(t)$ reduces its rotating frequency by $k\omega$. For instance, the k^{th} order harmonic is kept still and becomes a DC value; the $n=k+1$ and $n=k-1$ order harmonics rotate at the speeds ω and $-\omega$ (clockwise), respectively.

B. Step 2, Filtering

Calculating the mean value at $[-\pi, \pi]$, as (5) and (6), is equivalent to applying a proper low pass filter (LPF) to the outputs from step 1. A Moving Average Filter (MAF) is a good choice for removing all of the AC components, leaving the concerned k^{th} order harmonics in the DC form in the dq frame.

C. Step 3, Restoring Target Signal

The target harmonic can be restored by (7), which is the reverse process of step 1 and is actually a coordinate transform back to the original polar system. Only the target k^{th} order harmonic is restored because of the filtering in step 2.

The aforementioned process can be implemented as Fig. 4. It can be seen that the TOF-based method is directly applied to the single-phase signal in the polar coordinate system, which is different from the Park transform for 3-phase

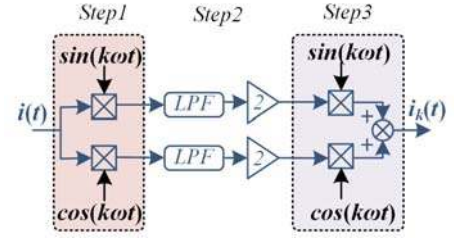


Fig. 4. Implementation of proposed TOF-based algorithm.

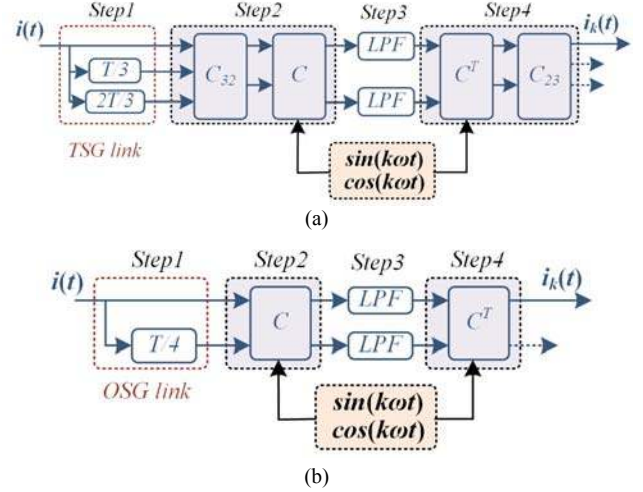


Fig. 5. Implementation of IRPT-based algorithm. (a) With TSG link; (b) With OSG link.

signals. Therefore, the two methods have totally different meaning and different expressions.

IV. COMPARISONS

In addition to accuracy, efficiency is another significant criterion to evaluate a harmonic extraction algorithm. To demonstrate the superiority of the proposed TOF-based algorithm in case of single-phase applications, comparisons with commonly used IRPT-based methods are provided in this section.

For single-phase applications, the conventional IRPT-based methods normally includes two stages, a VSG link and a Park transform, as depicted in Fig. 5. The additional VSG link can be realized by the TSG or OSG, depending on which coordinate the virtual signal is generated in.

For the TSG scheme in Fig. 5(a), two virtual signals are generated in the abc-stationary frame. This is normally accomplished by T/3 transport delays from each other, where T is the fundamental period. After the TSG link, a coordinate transform from the abc frame to the $\alpha\beta$ frame (as (9)) and a transform from the $\alpha\beta$ frame to the dq frame (as (10)) should be applied. Then the target harmonic is extracted through a LPF and inverse transforms.

$$C_{32} = C_{23}^T = \begin{bmatrix} 1 & -1/2 & -1/2 \\ 0 & \sqrt{3}/2 & -\sqrt{3}/2 \end{bmatrix} \quad (9)$$

TABLE I
COMPARISONS OF OCCUPIED RESOURCES

		Multiplier	Adder	Array
IRPT	TSG	18	13	5
	OSG	10	8	4
TOF		6	5	2

$$C = \begin{bmatrix} \cos(k\omega t) & \sin(k\omega t) \\ -\sin(k\omega t) & \cos(k\omega t) \end{bmatrix} \quad (10)$$

For the OSG scheme in Fig. 5(b), only one virtual in-quadrature-phase signal is directly generated in the $\alpha\beta$ frame, and multiple alternatives can be adopted to realize it, such as a T/4 transport delay [27]-[29], differential [30], Hilbert transform [31], inverse Park transform [32] or second order generalized integration [33]. Here, the simplest scheme, a T/4 transport delay, is employed for comparison.

From the point view of efficiency, straightforward comparisons can be made through Fig. 4 and Fig. 5(a) and 5(b). Obviously, the IRPT with the OSG is better than the scheme with the TSG, since the transform from the abc frame to the $\alpha\beta$ frame can be avoided. Meanwhile, the TOF-based method is superior to both of the IRPT-based methods, because the VSG link is avoided and the matrix operation during the Park transform is simplified.

For a detailed comparison, the computing resources occupied by the 3 types of schemes are listed in Table I, where the MAF is employed as a LPF in each scheme for a fair comparison. The data in Table I verifies the above analysis. The IRPT with the OSG occupies fewer resources than the TSG scheme, whereas the TOF-based method is the most efficient one, since it costs the least in terms of computing resources.

The efficiency of the proposed TOF-based algorithm can also be verified through the execution time in the digital signal processor. A DSP (TI TMS320F28335) is employed, and the practical execution times for extracting a single harmonic are compared in Fig. 6 for each algorithm. Obviously, the TOF-based method shows the fastest calculation, and this superiority is multiplied when several harmonics need to be extracted.

Actually, the IRPT-based method was originally designed for the 3-phase condition. Therefore, the VSG link is indispensable when it is used in single-phase applications. Even so, only one of the three outputs (for the TSG scheme in Fig. 5(a)) or one of the two outputs (for the OSG scheme in Fig. 5(b)) is valuable, while the others are abandoned. Moreover, considering VSG link, which is realized by a transport delay, would further decrease the response speed, the IRPT-based method is not an efficient one for single-phase applications. These are just the superiorities of the proposed TOF-based algorithm.

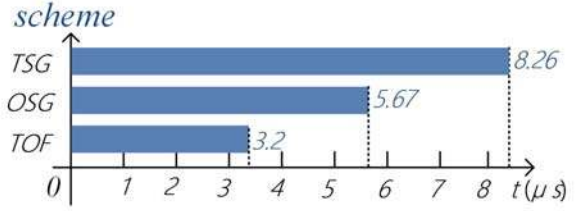


Fig. 6. Execution time comparison for single harmonic extraction

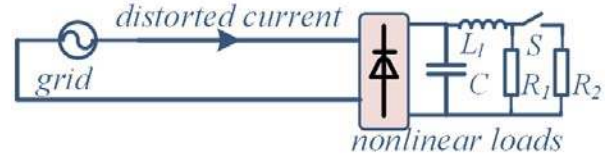


Fig. 7. Simulation model for distorted current generation.

TABLE II
PARAMETERS OF SIMULATION MODEL

DC capacitor	$C=500\mu F$
DC inductor	$L_1=0.01mH$
DC resistor 1	$R_1=10\Omega$
DC resistor 2	$R_2=5\Omega$
grid voltage	$V_{grid}=220V$
fundamental frequency	$f_1=50Hz$

V. VALIDATION

A. Simulation Verifications

Simulations are carried out in PSIM to verify the performances of the proposed TOF-based algorithm. For this purpose, a single-phase rectifier, with a DC-capacitor and resistors, is connected to the grid to generate distorted current. The detail configuration is shown in Fig. 7, and the corresponding parameters are listed in Table II.

This kind of nonlinear load generates a distorted current containing odd order harmonics, such as 1, 3, 5, 7.... In addition, the corresponding waveforms and spectrums are illustrated in Fig. 8. Additionally, a manual switch S is employed, as shown in the Fig. 7, to trigger a load step change at 0.10s, with which the transient response of the TOF-based algorithm can also be checked.

Taking fundamental component extraction as an example, Fig. 9 depicts the performances of the proposed TOF-based algorithm. The meanings of the DC- and AC- quantities on the d/q axis can be observed from Fig.4, where the DC quantities are doubled outputs of the LPF, and the AC quantities are multiplications of the DC quantities with corresponding phase information. The transient response can also be observed from Fig. 9, where the transient state is started at the moment of the load step-change and completely finished after one main cycle at most. This duration is mainly determined by the cut-off frequency of the LPF, and normally filtering fundamental component needs the longest time

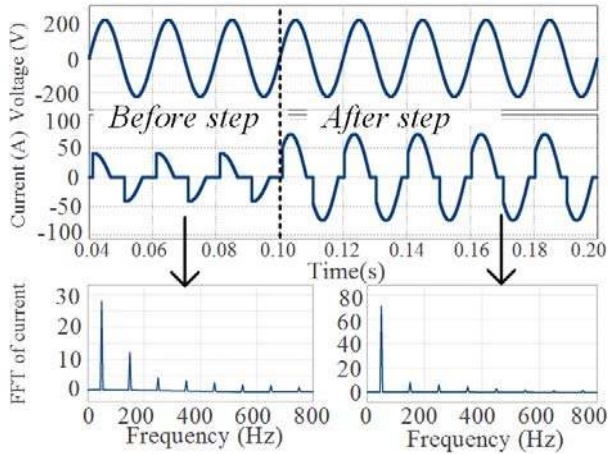


Fig. 8. Distorted current from single-phase nonlinear load.

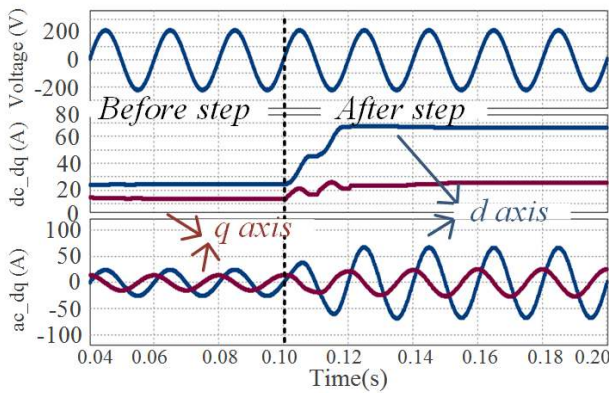


Fig. 9. Dc and ac quantities on d/q-axis with TOF based algorithm.

compared to the harmonics. In this test, the MAF with the window length of a fundamental period is employed as a LPF.

According to Fig. 4, the fundamental component can be obtained by summing up both the d-axis and q-axis AC quantities in Fig. 9, and the result is shown in the last line of Fig. 10. Comparing the magnitude of the extracted fundamental component in Fig. 10 and the fundamental value of the FFT spectrum regarding the original distorted current in Fig. 8, it can be seen that information about the target component is well extracted in the steady state for both the “before step” and “after step” conditions. Similar results can be also achieved when extracting the harmonic component, which validates the reasonability of the TOF-based algorithm.

B. Experimental Verifications

A laboratory prototype is established to validate the effectiveness of the proposed TOF based-algorithm. The configuration of the prototype is the same as that shown in Fig. 1, in which the shunt APF is a single-phase grid-connected H-bridge inverter and the nonlinear load is a controllable current source injecting the fundamental and 3rd, 5th, 7th order harmonic current into the grid. The corresponding main parameters of the prototype are listed in TABLE III.

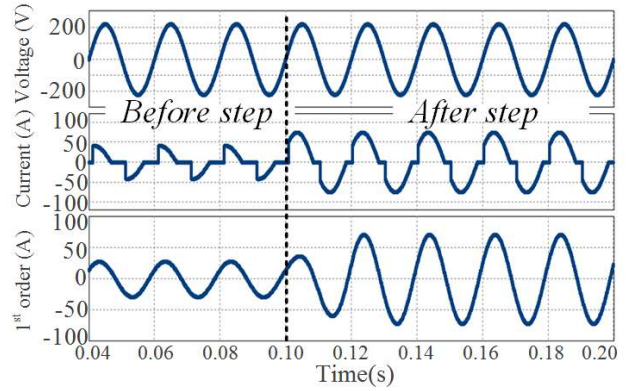


Fig. 10. Simulating result for fundamental component extraction.

TABLE III

PROTOTYPE PARAMETERS

grid voltage	$V_{grid}=220V$
DC-voltage	$V_{dc}=750V$
line inductor	$L=0.4mH$
switching frequency	$f_s=10kHz$
fundamental frequency	$f_1=50Hz$

Prototypes of single-phase APFs have already been tested in previous works. The only newly involved link is the harmonic extraction link, which is realized by the TOF-based algorithm. Therefore, the APF output current (i_o) can be directly regarded as amplified results of the TOF-based algorithm, and the effectiveness of the proposed algorithm can be verified through harmonics filtering performances. The corresponding experimental results are illustrated in Fig. 11-15.

Fig.11 depicts the distorted current from the controllable current source, which represents the distorted load current i_l . It contains 50A 1st order, 13A 3rd order, 13A 5th order and 13A 7th order components, with a total harmonic distortion (THD) reaching 48.6%. The corresponding FFT analysis is displayed at bottom of the figure, which indicates the specific content of the distorted current i_l .

Firstly, the harmonic selectivity of the TOF-based method is tested. Fig. 12 describes the condition where only the 3rd order harmonic is filtered. As expected, only the 3rd order harmonic current is output by the APF, as shown by i_o . In addition, the filtered source current (i_s) still contains 5th and 7th order harmonics but without the 3rd order harmonic, according to the FFT spectrum. In this condition, the THD of i_s drops to 38.5%. This test well validates the accuracy and selectivity of the TOF-based algorithm.

Similarly, in Fig. 13, the 3rd and 5th order harmonics are extracted by the TOF-based algorithm and are filtered through a single-phase APF. Again, the waveform and FFT analysis of i_s validate the effectiveness of the proposed algorithm. In addition, the THD of i_s comes to 25.3% in this case.

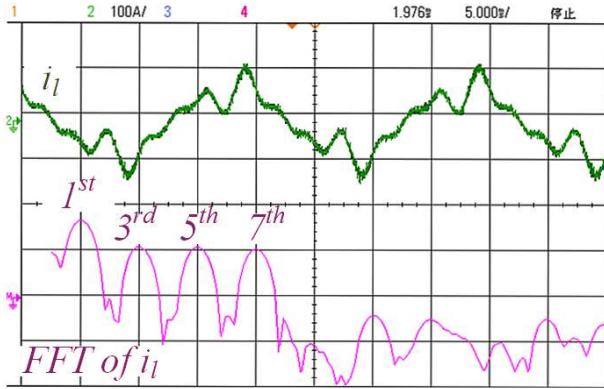


Fig. 11. Waveform and spectrum of distorted current. Scale for waveform: 100A/div, 5ms/div; scale for FFT: 20dB/div, 100Hz/div.

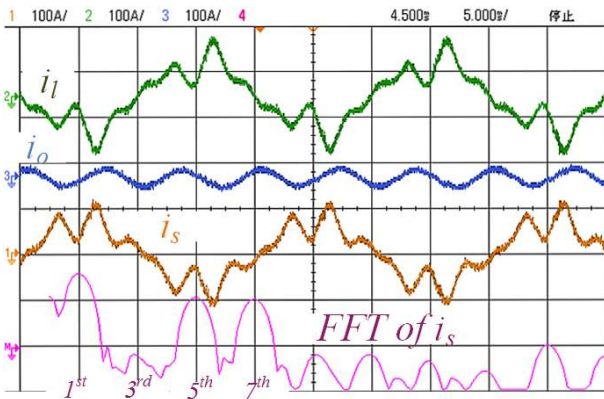


Fig. 12 Harmonics filtering performance with only 3rd order harmonic filtered. Scale for waveforms: 100A/div, 5ms/div; scale for FFT: 20dB/div, 100Hz/div.

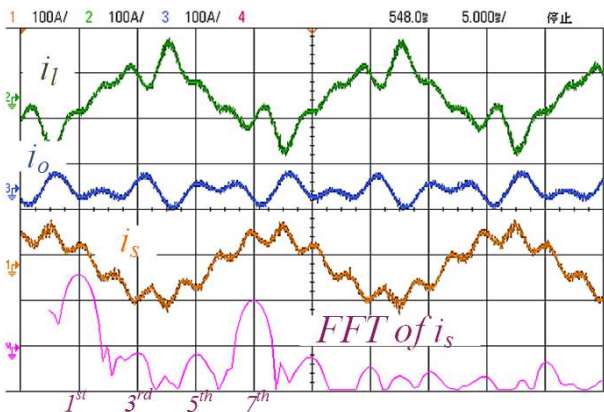


Fig. 13 Harmonics filtering performance with only 3rd and 5th order harmonics filtered. Scale for waveforms: 100A/div, 5ms/div; scale for FFT: 20dB/div, 100Hz/div.

Finally, all of the 3rd, 5th and 7th order harmonics are extracted and filtered in the third test, and the performance is depicted in Fig.14. As this figure shows, a good filtering result is obtained, and only the fundamental component is left after filtering, according to waveform and spectrum of i_s . In addition, the THD of i_s becomes 3.8% under this condition.

Additionally, the transient filtering performance is also

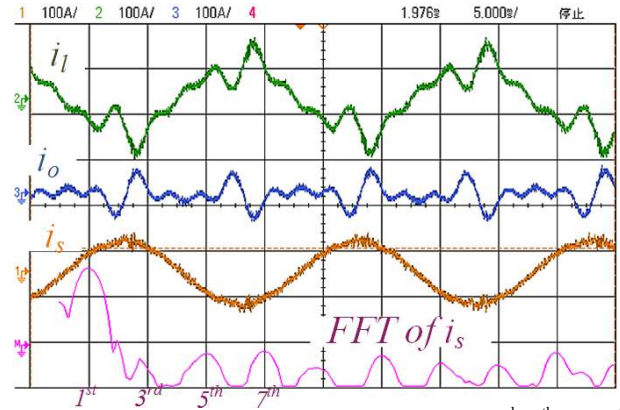


Fig. 14 Harmonics filtering performance with all 3rd, 5th and 7th order harmonic filtered. Scale for waveforms: 100A/div, 5ms/div; scale for FFT: 20dB/div, 100Hz/div.

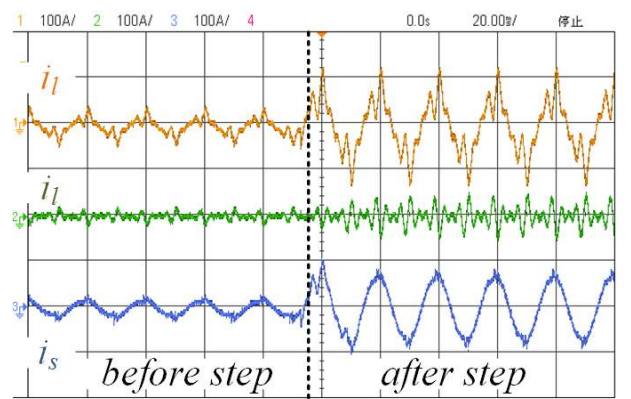


Fig. 15 Transient filtering performances. Scale for waveforms: 100A/div, 20ms/div.

tested by step-changing the distorted load current from 10A to 55A, and the result is depicted in Fig.15. As this figure shows, in addition to good filtering performances in the steady states, a fast response, with a transient state that is finished within one main cycle, is also achieved, which is identical to the simulation in Fig.9.

The above experimental results validate the accuracy, selectivity and rapid response of the proposed TOF-based harmonic extraction algorithm. Considering the additional benefit of a low computing cost, this TOF-based algorithm truly provides a preferable choice for single-phase APFs.

VI. CONCLUSIONS

This paper proposes a novel efficient harmonics extraction algorithm for single-phase APFs, based on the principle of Trigonometric Orthogonal Functions (TOF). Unlike the commonly used IRPT-based method, which needs a VSG link and a Park transform, the proposed TOF-based algorithm is directly applied to the single-phase signal, which greatly reduce the computing cost in terms of ensuring accurate and rapid harmonics extraction performances. The detailed mathematical principle and physical meaning are introduced,

and specific validations are carried out through simulations and laboratory experiments.

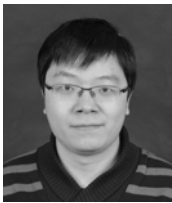
ACKNOWLEDGMENT

This work was supported by the National Natural Science Foundation of China under Grant 51507132, and also by the Power Electronics Science and Education Development Program of Delta Environmental and Educational Foundation under Grant DREG2015018.

REFERENCES

- [1] Q.-N. Trinh and H.-H. Lee, "An advanced current control strategy for three-phase shunt active power filters," *IEEE Trans. Ind. Electron.*, Vol. 60, No. 12, pp. 5400-5410, Dec. 2013.
- [2] P. Mattavelli and F. P. Marafao, "Repetitive-based control for selective harmonic compensation in active power filters," *IEEE Trans. Ind. Electron.*, Vol. 51, No. 5, pp. 1078-1024, Oct. 2004.
- [3] H. Yi, F. Zhuo, Y. Zhang, Y. Li, W. Zhan, W. Chen, and J. Liu, "A source-current-detected shunt active power filter control scheme based on vector resonant controller," *IEEE Trans. Ind. Appl.*, Vol. 50, No. 3, pp.1953-1965, May/June. 2014.
- [4] X. Wang, F. Blaabjerg, and Z. Chen, "Autonomous control of inverter-interfaced distributed generation units for harmonic current filtering and resonance damping in an islanded microgrid," *IEEE Trans. Ind. Appl.*, Vol. 50, No. 1, pp. 452-461, Jan./Feb. 2014.
- [5] J. He, Y. W. Li, F. Blaabjerg, and X. Wang, "Active harmonic filtering using current-controlled, grid-connected DG units with closed-loop power control," *IEEE Trans. Power Electron.*, Vol. 29, No. 2, pp. 642-653, Feb. 2014.
- [6] W. M. Grady, M. J. Samotij, and A. H. Noyola, "Survey of active power line conditioning methodologies," *IEEE Trans. Power Del.*, Vol. 5, No. 3, pp. 1536-1542, Jul. 1990.
- [7] L. A. Moran, J. W. Dixon, and R. R. Wallace, "A three-phase active power filter operating with fixed switching frequency for reactive power and current harmonic compensation," *IEEE Trans. Ind. Electron.*, Vol. 42, No. 4, pp. 402-408, Aug. 1995.
- [8] B. McGrath, D. Holmes, and J. Galloway, "Power converter line synchronization using a discrete Fourier transform (DFT) based on a variable sample rate," *IEEE Trans. Power Electron.*, Vol. 20, No. 4, pp. 877-884, Jul. 2005.
- [9] S. Gonzalez, R. Garcia-Retegui, and M. Benedetti, "Harmonic computation technique suitable for active power filters," *IEEE Trans. Ind. Electron.*, Vol. 54, No. 5, pp. 2791-2796, Oct. 2007.
- [10] E. Jacobsen and R. Lyons, "The sliding DFT," *IEEE Signal Process Mag.*, Vol. 20, No. 2, pp. 74-80, Mar. 2003.
- [11] E. Jacobsen and R. Lyons, "An update to the sliding DFT," *IEEE Signal Process Mag.*, Vol. 21, No. 1, pp. 110-111, Jan. 2004.
- [12] S. K. Jain, P. Agrawal, and H. O. Gupta, "Fuzzy logic controlled shunt active power filter for power quality improvement," *Proc. Inst. Elect. Eng.—Elect. Power Appl.*, Vol. 149, No. 5, pp. 317-328, Sep. 2002.
- [13] S. Liu, "An adaptive Kalman filter for dynamic estimation of harmonic signals," in *Proc. 8th Int. Conf. Harmonics Quality Power*, pp. 286-292, 1998.
- [14] S. Luo and Z. Hou, "An adaptive detecting method for harmonic and reactive currents," *IEEE Trans. Ind. Electron.*, Vol. 42, No. 1, pp. 85-89, Feb. 1995.
- [15] J. R. Varquez and P. Saimeron, "Active power filter control using neural network technologies," *Proc. Inst. Elect. Eng.—Elect. Power Appl.*, Vol. 150, No. 2, pp. 139-145, Mar. 2003.
- [16] L. Qian, D. Cartes, and H. Li, "Experimental verification and comparison of MAFC method and D – Q method for selective harmonic detection," in *Proc. IEEE 32nd IECON*, pp. 25-30, 2006.
- [17] M. Cirrincione, M. Pucci, G. Vitale, and A. Miraoui, "Current harmonic compensation by a single-phase shunt active power filter controlled by adaptive neural filtering," *IEEE Trans. Ind. Electron.*, Vol. 56, No. 8, pp. 3128-3143, Aug. 2009.
- [18] G. Chang, C.-I. Chen, and Y.-F. Teng, "Radial basis function based neural network for harmonic detection," *IEEE Trans. Ind. Electron.*, Vol. 57, No. 6, pp. 2171-2179, Jun. 2010.
- [19] W. Yifei and L. Yunwei, "Three-phase cascaded delayed signal cancellation PLL for fast selective harmonic detection," *IEEE Trans. Ind. Electron.*, Vol. 60, No. 4, pp. 1452-1463, Apr. 2013.
- [20] L. Asiminoaei, S. Kalaschnikow, and S. Hansen, "Overall and selective compensation of harmonic currents in active filter applications," in *Proc. CPE*, pp. 153-160, May 2009.
- [21] K. Sergej, L. Asiminoaei, and S. Hansen, "Harmonic detection methods of active filters for adjustable speed drive applications," in *Proc. 13th EPE*, pp. 1-10, Sep. 2009.
- [22] H. Akagi, "New trends in active filters for power conditioning," *IEEE Trans. Ind. Appl.*, Vol. 32, No. 3, pp. 1312-1322, May/June. 1996.
- [23] F. Z. Peng and J. S. Lai, "Generalized instantaneous reactive power theory for three-phase power systems," *IEEE Trans. Instrum. Meas.*, Vol.45, No. 1, pp. 293-297, Feb. 1996.
- [24] J. L. Willems, "A new interpretation of the Akagi-Nabae power components for nonsinusoidal three-phase situations," *IEEE Trans. Instrum. Meas.*, Vol. 41, No. 4, pp. 523-529, Aug. 1992.
- [25] H. Li, F. Zhuo, Z. Wang, W. Lei, and L. Wu, "A novel time-domain current-detection algorithm for shunt active power filters," *IEEE Trans. Power Syst.*, Vol. 20, No. 2, pp. 644-651, May 2005.
- [26] R. Bojoi, G. Griva, V. Bostan, M. Guerriero, F. Farina, and F. Profumo, "Current control strategy for power conditioners using sinusoidal signal integrators in synchronous reference frame," *IEEE Trans. Power Electron.*, Vol. 20, No. 6, pp. 1402-1412, Nov. 2005.
- [27] M. Karimi-Ghartemani, H. Mokhtari, M. R. Iravani, and M. Sedighy, "A signal processing system for extraction of harmonics and reactive current of single-phase systems," *IEEE Trans. Power Del.*, Vol. 19, No. 3, pp. 979-986, Jun. 2004.
- [28] J. Zhu, L. Li, and M. Pan, "Research on modular STATCOM based on dynamic reactive current detection method," in *Proc. of the 7th International Power Electronics and Motion Control Conference*, pp. 2760-2764, Jul. 2012.

- [29] S. Gautam, P. Yunqing, Y. Kafle, M. Kashif, S. UI-Hasan, "Evaluation of fundamental d-q synchronous reference frame harmonic detection method for single phase shunt active power filter," *International Journal of Power Electronics and Drive System (IJPEDS)*, Vol. 4, No. 1, pp. 112-126, Mar. 2014.
- [30] A. Luo, Y. Chen, Z. Shuai, and C. Tu, "An improved reactive current detection and power control method for single phase photovoltaic grid-connected DG system," *IEEE Trans. Energy Convers.*, Vol. 28, No. 4, pp. 823-831, Sep. 2013.
- [31] M. Saitou, N. Matsui, and T. Shimizu, "A control strategy of single-phase active filter using a novel d-q transformation," in *Proc. of the Industry Applications Conference 2003 (IAS'03)*, Vol. 2, pp. 1222-1227, Oct. 2003.
- [32] S. M. Silva, B. M. Lopes, J. C. Filho, R. P. Campana, and W. C. Bosventura, "Performance evaluation of PLL algorithms for single-phase grid-connected systems," in *Proc. of Industry Applications Conference 2004 (IAS'04)*, Vol. 4, pp. 2259-2263, Oct. 2004.
- [33] P. Rodriguez, R. Teodorescu, I. Candela, A. V. Timbus, M. Liserre, and F. Blaabjerg, "New positive-sequence voltage detector for grid synchronization of power converters under faulty grid conditions," in *Proc. of the IEEE Power Electronics Special Conference (PESC'06)*, pp. 1-7, 2006.

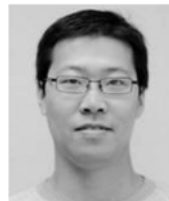


Hao Yi received his B.S. degree from the Hebei University of Technology, Tianjin, China, in 2007; and his M.S. and Ph.D. degrees from Xi'an Jiaotong University, Xi'an, China, in 2010 and 2013, respectively, all in Electrical Engineering. In 2013, he joined the School of Electrical Engineering of Xi'an Jiaotong University, as an Assistant Professor.

From 2016 to 2017, he was a Visiting Scholar in the Department of Energy Technology, Aalborg University, Aalborg, Denmark. His current research interests include the modeling and control of grid-connected converters, the control and power management of microgrids, and power quality improvement.



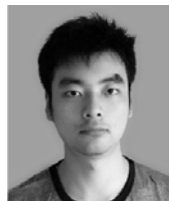
Fang Zhuo received his B.S. degree in Automatic Control, and his M.S. and Ph.D. degrees in Automation and Electrical Engineering from Xi'an Jiaotong University, Xi'an, China, in 1984, 1989, and 2001, respectively. He was a Visiting Scholar with the Nanyang Technological University, Jurong West, Singapore, in 2004. He has been a Full Professor of Power Electronics at Xi'an Jiaotong University, since 2004, where he is presently working as the Dean of the Faculty of Industry Automation. He has authored over 160 publications. His current research interests include power quality improvements and inverters for distributed power and power generation.



Feng Wang received his B.S., M.S., and Ph.D. degrees in Electrical Engineering from Xi'an Jiaotong University, Xi'an, China, in 2005, 2009, and 2013, respectively. He was an Ph.D. Exchange Student with the Center for Power Electronics Systems, Virginia Polytechnic Institute and State University, Blacksburg, VA, USA, from 2010 to 2012. He joined Xi'an Jiaotong University as Assistant Professor, in 2013. His current research interests include dc/dc conversion and the digital control of switched converters, especially in the field of renewable energy generation.



Yu Li received his M.S. degree in Electrical Engineering from Xi'an Jiaotong University, Xi'an, China, 2013. He is presently working at the Xi'an Spread Power Electric co. ltd, Xi'an, China, as the CTO. His current research interests include the control, design, and application of active power filters.



Zhenxiong Wang received his B.S. degree in Electrical Engineering from Xi'an Jiaotong University, Xi'an, China, in 2014, where he is presently working towards his PhD in the Department of Electrical Engineering. His current research interests include power quality and the control of distributed generation in microgrids.